



Fabrication of high-performance pervaporation desalination composite membranes with study of its acid-base stability

Menghan Yang^a, Chenghao Niu^a, Yifei Guo^b, Bing Cao^{b,*}, Rui Zhang^{b,*}

^a College of Materials Science and Engineering, Beijing University of Chemical Technology, Beijing 100029, China

^b College of Chemical Engineering, Beijing University of Chemical Technology, Beijing 100029, China

ARTICLE INFO

Editor: Dr. B. Van der Bruggen

Keywords:

Perfluorosulfonic acid
High performance pervaporation membrane
Membrane forming structure and mechanism
Concentration of acid and base solutions

ABSTRACT

In the process of industrial production will produce a lot of acid and alkaline waste liquid, how to effectively treat acid and alkali waste liquid is an important topic at present. At present, there are some problems about the treatment of acid and alkali waste liquid, such as large investment, complicated process and low efficiency. Pervaporation has the characteristics of mild operating conditions and no influence of osmotic pressure threshold, so it has great application potential in the concentration, reuse and reduction of acid and alkali waste liquid. However, at present, conventional pervaporation dense membrane materials cannot maintain long-term stability in strong acid and alkali environment, in order to achieve this performance, we use perfluorosulfonic acid resin with good acid and alkali resistance as the dense layer substrate. PFSA/PTFE/PP composite membrane was prepared by spraying process, and the final prepared composite membrane had a pure water flux of 45 ± 1.2 kg/(m²•h) at 70 °C. The acid and alkali resistance of the intrinsic membrane and the composite membrane was evaluated, and it was found that the feed liquid was concentrated to 20 wt% after 19 h long concentration operation at 70°C and starting liquid was 5 wt% H₂SO₄ and 5 wt% NaOH. The retention rate of acid and alkali can be maintained above 99.9 %. During the concentration of H₂SO₄ solution, the dense layer structure is affected, and the pure water flux of the composite membrane is reduced, eventually maintaining around 32 kg/(m²•h). In the process of concentrating NaOH solution, the pure water flux of the composite membrane increased first and then decreased, and the final pure water flux of the membrane remained near 40 kg/(m²•h).

1. Introduction

With the continuous and rapid growth of China's economy, the continuous improvement of the level of industrialization, and the rapid development of various industries, a large number of waste acids and alkalis are generated [1,2], and the waste liquid containing acids or alkalis cannot be directly discharged. First, the waste acids and alkalis will cause corrosion damage to equipment and pipelines in the process of discharge, and secondly, it will cause serious burden on the ecological environment [3–5]. In addition, the acid and alkali in the waste liquid can be reused as an important resource, and the direct discharge is a waste of acid and alkali resources. Therefore, the treatment of waste acid and waste alkali has been paid more and more attention, and the recycling of these two has become more and more urgent.

The current treatment methods for waste acid and alkali mainly include acid-base neutralization, evaporation concentration, diffusion dialysis, electrodialysis, membrane distillation, solvent extraction

[6–12], etc. At present, there are some shortcomings in the treatment of acid and alkali waste liquid, such as complicated process, high equipment cost, wide equipment area, low recovery rate and poor separation effect [13–16]. As a membrane treatment technology with high separation effect, pervaporation can not only concentrate and recycle the acid and base waste liquid, but also produce certain available water resources in this process, which is also a kind of saving of water resources [17–19].

Pervaporation is a membrane separation process that combines the process of osmosis and vaporization [20–22]. The migration process on both sides of the membrane is a solution-diffusion process, and the driving force of this migration is the chemical potential difference between the membranes. Pervaporation membrane is a non-porous membrane, and its separation characteristics are not dependent on relative volatility, but on the relative rate of penetration through the membrane, which is based on the affinity with the membrane material. In the process of contact between the membrane and the solution,

* Corresponding authors.

E-mail addresses: bcao@mail.buct.edu.cn (B. Cao), zhangrui1@mail.buct.edu.cn (R. Zhang).

<https://doi.org/10.1016/j.seppur.2024.129277>

Received 7 July 2024; Received in revised form 18 August 2024; Accepted 19 August 2024

Available online 19 August 2024

1383-5866/© 2024 Elsevier B.V. All rights are reserved, including those for text and data mining, AI training, and similar technologies.

molecules with high affinity are adsorbed and diffused through the membrane, while molecules with low affinity are retained by the membrane [23]. The dense, non-porous membrane has high selectivity, and the raw material liquid can be separated through the partial vaporization process of the components of the raw material liquid, and a high-purity penetrant can be collected [24]. The feed side of pervaporation is in a state of atmospheric pressure, while the permeation side is in a state of vacuum or scavenging. The PV test device commonly used in laboratories adopts the vacuum method to maintain the constant pressure on the permeation side [25]. The membranophilic components in the feed liquid exist in the form of gas phase after passing through the membrane, and a cold trap with rapid condensation or deposition of steam should be installed on the downstream side to collect the gas components for the purpose of analyzing the permeability and separability of the membrane [26]. In general, the permeability of the membrane is described using the flux method, which describes the weight of the mass passing through the membrane per unit of membrane area in unit time [27].

At present, the application and development of pervaporation is mainly concentrated in seawater desalination [28–31], where the salt retention rate is basically above 99.5 %, so the specific direction of research is to improve the osmotic flux in the process of pervaporation desalination. Pervaporation (PV) membrane separation technology is an environmentally friendly and highly selective new water treatment technology, which is the current research hotspot and the frontier direction of the development of water treatment field. In recent years, the technology has been increasingly applied in seawater desalination, which is an exploitable field for the concentration and reuse of acid and base. Its characteristics and advantages can meet the current vacancy in low-energy acid and base concentration and can also reduce waste liquid. However, PV technology is currently limited by the instability of membrane materials in acid-base environment, easy contamination of membrane and low membrane flux. There are few applications in the recovery and utilization of acid and alkali wastewater [32], mainly to study the resistance of the membrane in acid and alkali environment. Cui [33] prepared a series of acid-resistant polysulfone amide/polyether sulfone pervaporation composite membranes by interfacial polymerization. After soaking the membrane in 20 wt% H_2SO_4 solution for one week, the NaCl retention rate did not decrease. In addition, the water flux was stable in a 10 h pervaporation test at 75 °C using 10 wt% sulfuric acid solution as the feed. Bai [34] used polyethylene microfiltration membrane as substrate to deposit sodium layer of glutaraldehyde crosslinked carboxymethyl cellulose by spraying method. When 3.5 wt% sodium chloride solution was separated at 70°C, the pervaporation flux of the composite membrane reached 35 kg/($\text{m}^2\cdot\text{h}$), and the removal rate of sodium chloride was 99.9 %. After soaking in 20 wt% NaOH solution for 9 h and 10 wt% NaOH solution at 60°C for 80 h, the desalting performance of the membrane was stable. When 5 to 10 wt% of NaOH solution was concentrated at 60°C, the average water flux was 23 kg/($\text{m}^2\cdot\text{h}$), and the NaOH removal rate was over 99.98 %. Therefore, it is necessary to find acid-alkali resistant materials as the dense layer of PV composite membrane and improve the membrane-making method to improve the flux of the membrane and the efficiency of acid-base concentration on the premise of ensuring the good acid-alkali resistance of the membrane.

Perfluorosulfonic acid (PFSA) is a polymer polyelectrolyte with polytetrafluoroethylene (PTFE) molecular skeleton structure and $-\text{SO}_3\text{H}$ group at the end of the side chain [35]. In the structure of PFSA the carbon-fluorine bond has shorter bond length and higher bond energy, and the fluorine atom of the electric-rich group is larger than that of the hydrogen group, and its degree of polarization is smaller [36–38]. Coupled with the change of its molecular structure, the fluorine atom is tightly wrapped in the carbon-carbon main chain, thus forming a protective membrane of low fluorine atom on its surface. Thus, it has excellent thermal and chemical properties. The side chain of ionic polymers is fixed to the main chain by ether bond, and the end group is a

sulfonic acid group with hydrophilic properties [39], but perfluorinated materials do not exhibit particularly excellent properties in terms of hydrophilicity and water penetration rate due to their low surface tension [40]. PFSA has good chemical stability and hydrophilic mass transfer group ($-\text{SO}_3\text{H}$), which can be used as the base material of the dense layer of acid-base waste liquid in PV process. It is necessary to optimize the preparation process during the preparation of the dense layer and explore the modification of the hydrophilicity of the material in order to improve the water permeability of the membrane.

2. Experimental

2.1. Materials

Perfluorosulfonic acid (PFSA) was obtained from Dongyue Federation (China) and diluted it with deionized water to a concentration of 2 wt%. Concentrated H_2SO_4 (98 %) was bought from Tianjin Damo Chemical Reagent Factory (China). NaOH (analytically pure) were purchased from Tianjin Fuchen Chemical Reagent Factory (China). Deionized (DI) water ($13 \mu\text{s}/\text{cm} \leq \sigma \leq 20 \mu\text{s}/\text{cm}$) was manufactured from a laboratory-equipped RO water system. The support layer was PTFE/PP microfiltration membrane from membrane Solutions with an average membrane pore size of 0.22 μm (America).

2.2. Preparation of the PFSA/PTFE/PP composite membranes

PTFE/PP with flat surface, no defects and no scratches were selected as the composite membrane support layer, and the size was cut to 4 cm \times 4 cm. The support layer was submerged in an ethanol/water mixture and subjected to ultrasonic cleaning for 30 min. After the supporting layer is cleaned and dried, the membrane center size of 3.5 cm \times 3.5 cm is selected as the actual spraying area, and the surrounding area is pasted on the glass plate with cut aluminum foil tape.

Take 5 g of PFSA solution with a concentration of 20 wt%, add 45 g of deionized water to dilute the original solution to a PFSA solution with a concentration of 2 wt%, and stir until the spraying solution is evenly mixed. Take the clean support layer, paste aluminum foil tape into a 3.5 cm \times 3.5 cm box as the actual spraying area. Adjust the pipette indicator to 400 μL , adjust the appropriate spraying pressure, take a certain amount of spraying liquid in the spray pen spray can, and keep the distance between the spray pen and the support layer at about 10 cm. The spraying process should be ensured to be slow and even. After spraying, the five membranes with the same spraying amount were placed in a vacuum oven at 140°C and heated for 10 h, 12.5 h, 15 h, 17.5 h and 20 h, respectively (Fig. 1).

2.3. Characterizations

2.3.1. Hydrophilic analysis

The dynamic water contact Angle of the composite membrane. Water contact Angle measuring instrument (JC2000D Powereach China) was used to compare different post-treatment conditions to obtain the hydrophilicity of the membrane. During the measurement, one frame was set to be taken every 1 min.

Take 3.5 ± 0.005 g free-standing PFSA membrane as sample and place it in a beaker and soak it in water. The free-standing PFSA film was prepared on the glass panel by the same spraying process as described in Section 2.2. The measurement process was heated in an oven with a set temperature of 70°C and a time of 24 h. After cooling to room temperature, the sample was taken out, the surface water of the sample was quickly absorbed, and the mass of the membrane after water absorption balance was weighed by an analytical balance, which was recorded as m_1 . Then the sample membrane was placed in a vacuum oven and vacuum was extracted to dry it to constant weight, then the membrane was removed and weighed, and the mass was recorded as m_0 . The water content (W, %) is calculated by the following Equation (1):

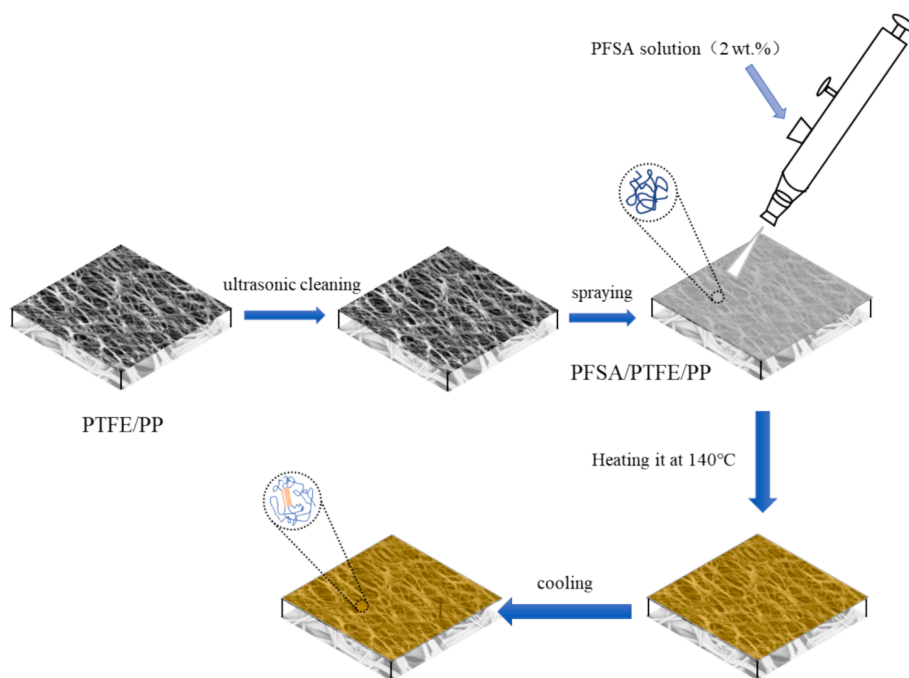


Fig. 1. A schematic diagram showing the method of preparing the PFSA/PTFE/PP composite membrane.

$$W = \frac{m_1 - m_0}{m_0} \times 100\% \quad (1)$$

2.3.2. Pervaporation flux test

The pervaporation test device in Fig. 2 was used to test the pure water flux of the composite membrane. The conditions required for the operation of this experiment are to keep the temperature of the raw material liquid at 70°C, the rotational speed of the peristaltic pump at 400 r/min, the pressure of 0.1 MPa for the permeation measurement of the membrane, the Reynolds number is 4700, and the liquid flow state on the surface of the membrane is turbulence state. The effective area of the composite membrane is 3.14 cm². During operation, liquid nitrogen is used to condense water vapor.

During this process, the water flux of the composite membrane (J : kg/(m²·h) is represented by Equation (2):

$$J = \frac{m}{At} \quad (2)$$

Where m is the mass of permeate (kg); A is the effective area of the membrane (m²); and t is the testing time (h).

2.3.3. Experimental process of concentration of H₂SO₄ solution and NaOH solution

In this section, 5 wt% H₂SO₄ solution was used as the feed stock test solution in the acid enrichment process, and 5 wt% NaOH solution was used as the feed stock test solution in the alkali enrichment process.

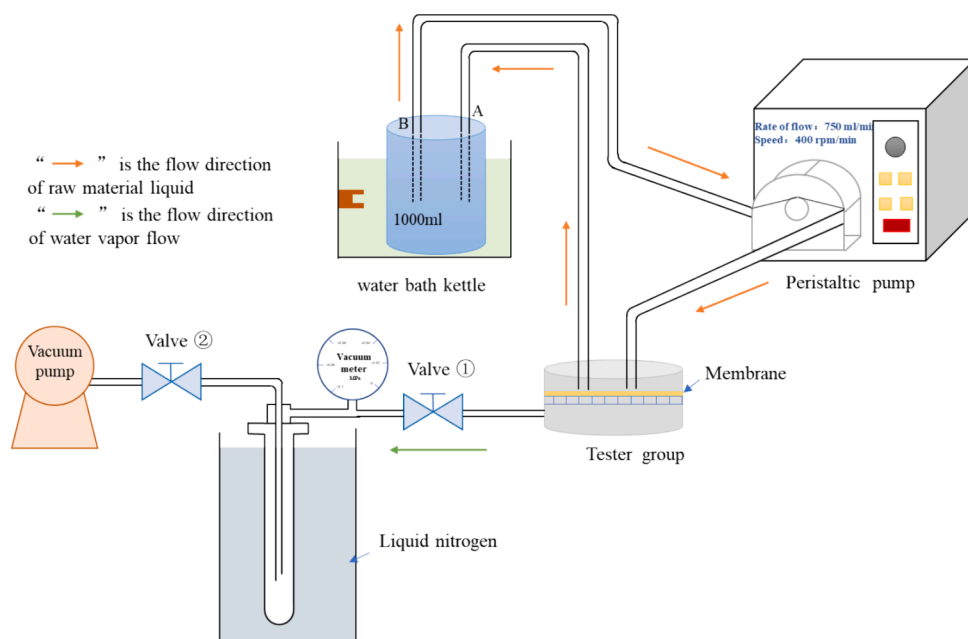


Fig. 2. The test equipment for pervaporation experiment.

Refer to the previous section for test conditions and procedures, and the water flux in the test process is calculated by Equation (2). The calculation formula of rejection (R : %) is expressed by Equation (3):

$$R = \frac{C_f - C_p}{C_f} \quad (3)$$

Where C_f is the conductivity of the feed solution before flux measurement, and C_p is the conductivity of water collected during PV operation. Before measuring the conductivity of water collected, the back of the membrane is washed with the collected water to wash the acid or alkali away from the back of the membrane, which can better reflect the membrane's barrier effect on acid and alkali.

2.3.4. SEM surface and cross-section morphology observation

Thermal field emission scanning electron microscope (HITACHI S-7800 Japan) was used to observe the cross section and surface morphology of PFSA/PTFE/PP composite membrane before and after PV acid base concentration test. To observe the section morphology, the sample should be brittle in liquid nitrogen. The Nano Measurer software was used to measure the thickness of the PFSA layer. The surface of all samples shall be treated with gold spraying before SEM testing.

2.3.5. FTIR structural analysis

The Transmission E.S.P. in the FTIR Spectrometer (Nicolet iS50, Thermo Scientif) was used to characterize whether the chemical structure of the membrane changed after soaking in acid-based solution. The test wave number ranges from 400 cm^{-1} to 4000 cm^{-1} and the resolution is set at 8 cm^{-1} .

2.3.6. XRD crystalline analysis

XRD characterization Using X-ray diffractometer (XRD, tall Ultima IV, Rigaku, Japan) to the analysis under the action of acid and alkali, the crystallinity of the free-standing PFSA membrane and grain size change, test point for $5 \sim 35^\circ$, scan rate is 1% min. Selection of preparation conditions of the same three membrane to measure its XRD spectrum diagram, determine its after 70°C respectively, in $20 \text{ wt}\% \text{ H}_2\text{SO}_4$ solution after soaking XRD spectra; Selection and preparation conditions of the same three membrane after determination of the XRD spectra, and measure its after 70°C and $20 \text{ wt}\% \text{ NaOH}$ solution after soaking XRD spectra. Select three membrane purpose is to reduce experimental error.

XRD analysis of PFSA dense membranes shows overlapping peaks from crystalline and amorphous regions, so it is necessary to use Gaussian peak division method to distinguish the two, as shown in

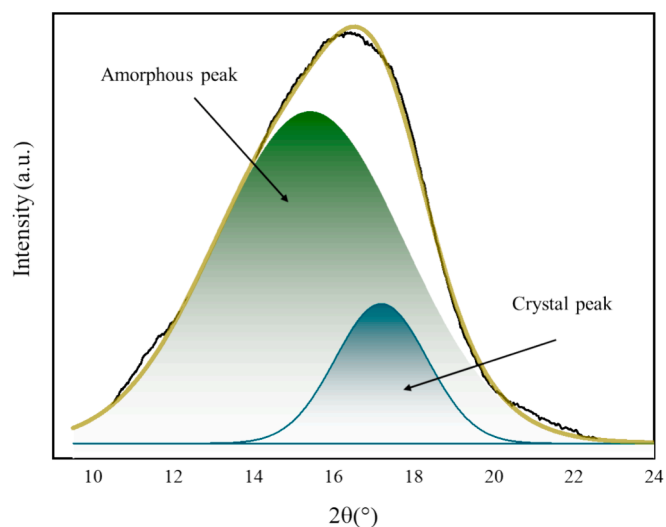


Fig. 3. Schematic diagram of XRD peak Gauss peak-splitting method for PFSA membrane.

Fig. 3. After peak separation, the weight crystallinity can be obtained by comparing the diffraction pattern intensity of the crystal region with the total scattering intensity, which is expressed by Equation (4).

$$f_c^w = \frac{\int_0^\infty s^2 I_c(s) ds}{\int_0^\infty s^2 I(s) ds} \quad (4)$$

Where, f_c^w is the calculated crystallinity, I_c is the intensity of the diffraction pattern in the crystal region, which is about 17.5° , I is the total scattering intensity, and s is the scattering vector, which is expressed by Equation (5).

$$s = \frac{2\sin(\theta)}{\lambda} \quad (5)$$

Where, θ is the diffraction Angle and λ is the wavelength of the X-ray, which in this experiment is 0.15406 nm .

The crystallization properties of PFSA are mainly determined by the polytetrafluoroethylene segment, and the half-peak width of the crystallization peak in the diffraction peak in this experiment is larger than that of polytetrafluoroethylene. Two factors of crystal peak broadening are considered: lattice distortion and grain refinement. In this experiment, it is assumed that the main factor leading to crystal peak broadening is the refinement of crystal particles. The grain size is expressed by Equation (6), namely Scherrer's formula.

$$t = \frac{K\lambda}{B\Delta \cos\theta} \quad (6)$$

Where, t is the grain size; B is the half-peak width of the measured crystal peak, which is converted into radians in calculation; K is Scherrer's constant, $K=0.89$; λ is the X-ray wavelength; θ is the 2θ Angle of the crystal peak, unit is the Angle.

2.3.7. XPS

X-ray spectroscopy (XPS, ESCALAB 250, THERMO VG, USA) was used to characterize the surface element changes of PFSA membranes after alkali immersion. The prepared PFSA membrane was treated with gold spray, and the composition of elements on the surface of the membrane was measured before and after soaking in $20 \text{ wt}\% \text{ NaOH}$ solution, and the influence of alkali on the composition of elements on the surface of the membrane was analyzed. In this test, ultra-pure water should be used to soak and clean the membrane after the alkaline solution is soaked, and the ultra-pure water should be replaced once 10 min . When the pH value of the ultra-pure water immersion solution is stable at $6.8 \sim 7$, it is confirmed that the alkali solution in the membrane is cleaned totally.

2.3.8. DMA

A dynamic thermomechanical analyzer (DMA, Q-800, TA, USA) was used to determine the tensile properties of the free-standing PFSA membrane. The test mode was set to allow the tensile force to increase slowly at a speed of 0.2 N/min until the film was fractured.

2.3.9. TGA

Thermogravimetric analysis (TGA, HTG-1, Beijing) was used to characterize the thermal stability of the free-standing PFSA membrane after soaking in acidic and alkaline solution. The test was carried out in N_2 atmosphere, the temperature range was 25°C to 900°C , and the heating rate was set at 10°C/min . The 30 mg intrinsic film was evenly divided into three parts, each 10 mg , one part was used as the original film to be tested, one part was soaked in $20 \text{ wt}\% \text{ NaOH}$ solution for 300 h , and the other part was soaked in $20 \text{ wt}\% \text{ H}_2\text{SO}_4$ solution for 300 h .

3. Result and discussion

3.1. Effect of annealing duration on microstructure and properties of membrane

3.1.1. The change of XRD pattern

The spraying process of the dense layer can make the polymer droplets fall on the PTFE fiber layer and surface, and then the solution evaporates into a membrane, forming a PFSA membrane on the PTFE surface. The PFSA membrane after spraying is tested by XRD, as shown in Fig. 4. The amorphous region ($2\theta \approx 15.5^\circ$) and crystal region ($2\theta \approx 17.5^\circ$) detected by XRD were fitted to separate peaks, and the crystallinity was calculated to be 5.03 %, at which time the crystal region in PFSA membrane was very small. Therefore, the performance of the membrane at this time is poor solvent resistance, and it is easily dissolved in water, so it can not be used for the pervaporization process, so the membrane needs to be treated at 140°C .

Fig. 5 shows the XRD test results of PFSA dense membranes under different annealing duration. It can be seen from the figure that two diffraction peaks can be obtained for each membrane in the diffraction Angle range of $6\text{--}25^\circ$, among which the diffraction peak of about 15.5° is caused by signals from the amorphous region in the membrane. The diffraction peak of about 17.5° is due to the signal of the crystal region in the membrane.

After dividing the Gaussian peaks of the curve in Fig. 5, Table 1 can be obtained by calculating according to Equation (5) and (6). It can be seen that with the extension of annealing time, the crystallinity and grain size of the dense PFSA layer increase continuously. This is because in the annealing process of PFSA membrane at 140°C , the molecular chain segment has the ability to move fully at this time, the longer the annealing time, the more the chain segment movement, the more the crystal region can be further grown, and the degree of lamellar thickening is more obvious, which is reflected in the improvement of crystallinity. In addition, the process of crystal lattice improvement will also occur during the annealing process. Some small and imperfect crystal structures in PFSA membrane will be destroyed during the continuous extension of heating time, forming a more perfect crystal structure, and the movement of molecular chain segments will promote the elimination of the internal stress in the crystal region, the amorphous region, and the interface region between the amorphous region and the crystal region. The increase of grain size is promoted as well.

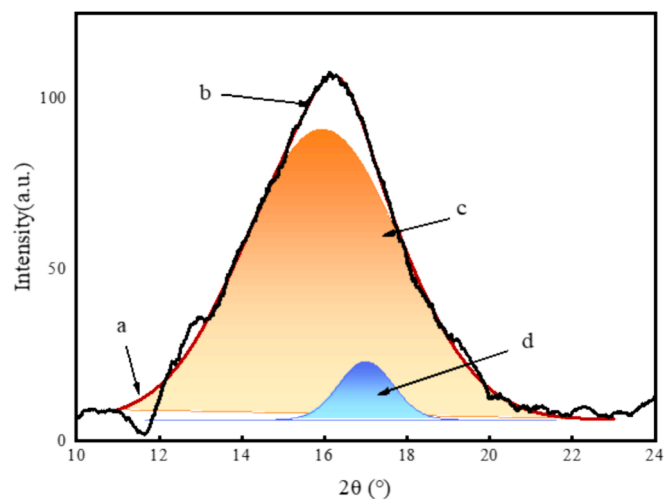


Fig. 4. XRD pattern of spraying membrane, in which (a) is the cumulative peak fitting line, (b) is the XRD detection peak, (c) is the amorphous peak, and (d) is the crystallization peak.

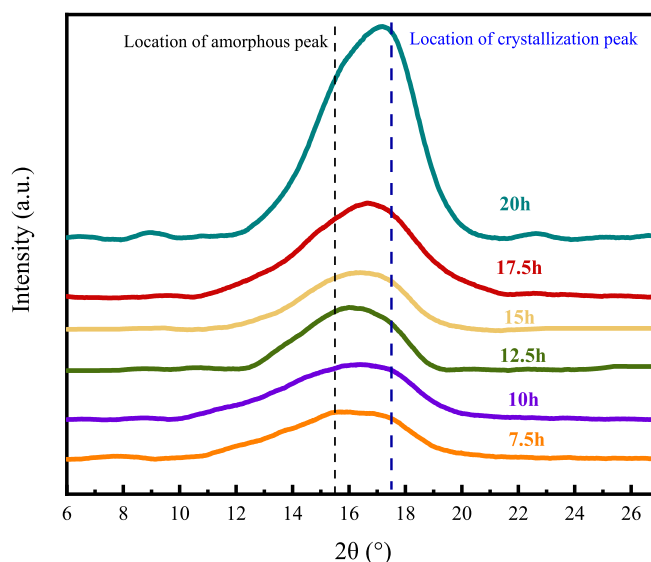


Fig. 5. XRD pattern of different annealing time.

Table 1

The crystallization properties of the membranes changed with different annealing time.

Annealing duration (h)	Degree of crystallinity (%)	Half-peak width ($^\circ$)	The average size of grains (nm)
7.5	15.83	3.13	2.63
10	16.30	2.82	2.92
12.5	16.81	2.63	3.13
15	17.30	2.58	3.19
17.5	17.36	2.13	3.86
20	17.79	2.09	3.94

3.1.2. Hydrophilicity of PFSA membrane at different treated time

Figure above indicates, the longer the annealing time, the more obvious the water content of the dense layer decreases, which indicates that the hydrophilicity of the dense layer decreases continuously during the process. In the test of the water contact Angle on the surface of the composite membrane, the change of the contact Angle in the early stage is affected by the hydrophilicity of the dense layer, resulting in different degrees of membrane infiltration. However, when the water infiltration reaches a certain degree, the water contact Angle on the surface of the membrane no longer shows a linear change trend, so the measurement of dynamic contact Angle only takes the linear change value in the first 15 min. After linear fitting of each group of data, the absolute value of the slope keeps decreasing. Under the same test conditions, in each group of tests, water droplets volatilize to air at a similar rate, and the difference in absolute slope values is mainly influenced by the diffusion speed of water into the dense layer. As shown in Table 2, the absolute value of the slope after fitting also keeps decreasing with the extension of annealing time, and the reduction degree of contact Angle also keeps decreasing, which indicates that the diffusion rate of water to the inside

Table 2

Absolute slope value of fitted line in Fig. 6(c).

Annealing duration (h)	Absolute value of slope
7.5	1.72338 ± 0.03468
10	1.47137 ± 0.05181
12.5	1.16106 ± 0.02455
15	1.01922 ± 0.0356
17.5	0.9364 ± 0.04304
20	0.92137 ± 0.04579

of the dense layer decreases during the extension of annealing.

The effect of annealing time on the hydrophilicity of the compact layer is essentially determined by the difference of the internal structure of the PFSA layer, that is, the difference of the crystalline structure within the membrane. For the infiltration of water molecules in the dense layer of the PV process, it is generally believed that the infiltration efficiency of water in the crystallization zone is extremely low, and the water infiltration process mainly occurs in the amorphous zone. The increase of crystallinity and grain size will also lead to a decrease in the hydrophilicity of PFSA and the mass transfer efficiency of water molecules. This is because the dimensional stability of the PFSA layer increases the limit of the swelling of the dense layer, resulting in a decrease in the permeability of the dense layer to water, resulting in a decrease in the water content of the membrane, the contact Angle and the pure water flux.

3.1.3. Tensile properties of PFSA membrane at different treated time

It can be seen from the Fig. 7 that the tensile strength increases with the extension of annealing time, the tensile strength of PFSA membrane increases continuously, and the elongation at break increases first and then decreases. When the annealing time was 12.5 h, PFSA membranes showed good tensile strength and elongation at break.

The effect of annealing time on the mechanical properties of the dense layer is also reflected by the difference of the crystalline structure inside the PFSA layer. When the crystallinity of the membrane increases, the tensile strength of the material is improved. When the annealing time is short, the crystallinity and grain size of the membrane are too low, and the crystallization sites inside the membrane are few and unstable, resulting in low tensile strength and elongation at break. When the annealing time is prolonged, the crystallization property is enhanced, the tensile strength is increased, and the elongation at break is increased. However, if the crystallinity is too high, the elongation at break of the material will decrease and the brittleness of the material will increase. In addition, too large grain size will also lead to the reduction of the elongation at break of the material, the toughness of the material is reduced, and the ductility of the membrane is not good.

The annealing time makes the structure of the membrane different in terms of crystallization properties. Overall, the selection of annealing time conditions first from the perspective of hydrophilicity, the annealing time of the membrane should not be too long, which is unfavorable to the water penetration efficiency of the PV process; Secondly, it is considered from the strength and toughness of the membrane, because the pervaporation process in the swelling and osmotic vacuum conditions to ensure the integrity and density of the membrane, so there are certain requirements for the strength and toughness of the membrane, and the annealing time of the membrane cannot be too long or too short. By comparing the pure water flux, dynamic contact angle and tensile properties of the membranes, it can be determined that the overall performance of the composite membrane is the best when the annealing time is 12.5 h, and the pure water flux is $45 \pm 1.2 \text{ kg}/(\text{m}^2 \cdot \text{h})$. In order to ensure that the membrane has certain mechanical properties, we choose a spray volume of 1.2 ml.

3.2. Evaluation of acid resistance of composite membrane

3.2.1. Effect of H_2SO_4 on the structure of dense layer

Fig. 8(a) shows the infrared spectrum changes of PFSA with annealing duration of 12.5 h during the H_2SO_4 immersion process. It can be seen that during the immersion of PFSA dense layer with H_2SO_4 , the peaks around 1210 cm^{-1} and 1060 cm^{-1} are the stretching vibration of $-\text{SO}_3^-$ group, and 980 cm^{-1} and 960 cm^{-1} are the symmetric stretching vibration of C-O-C group. After 72 h immersion, the shape and intensity of the peaks hardly changed, which indicated that H_2SO_4 did not cause the destruction and fall of hydrophilic groups in the membrane, and the molecular chain structure of PFSA could remain intact in H_2SO_4 . However, during 0–4 h soaking, the absorption peak of $-\text{SO}_3^-$ moved to a

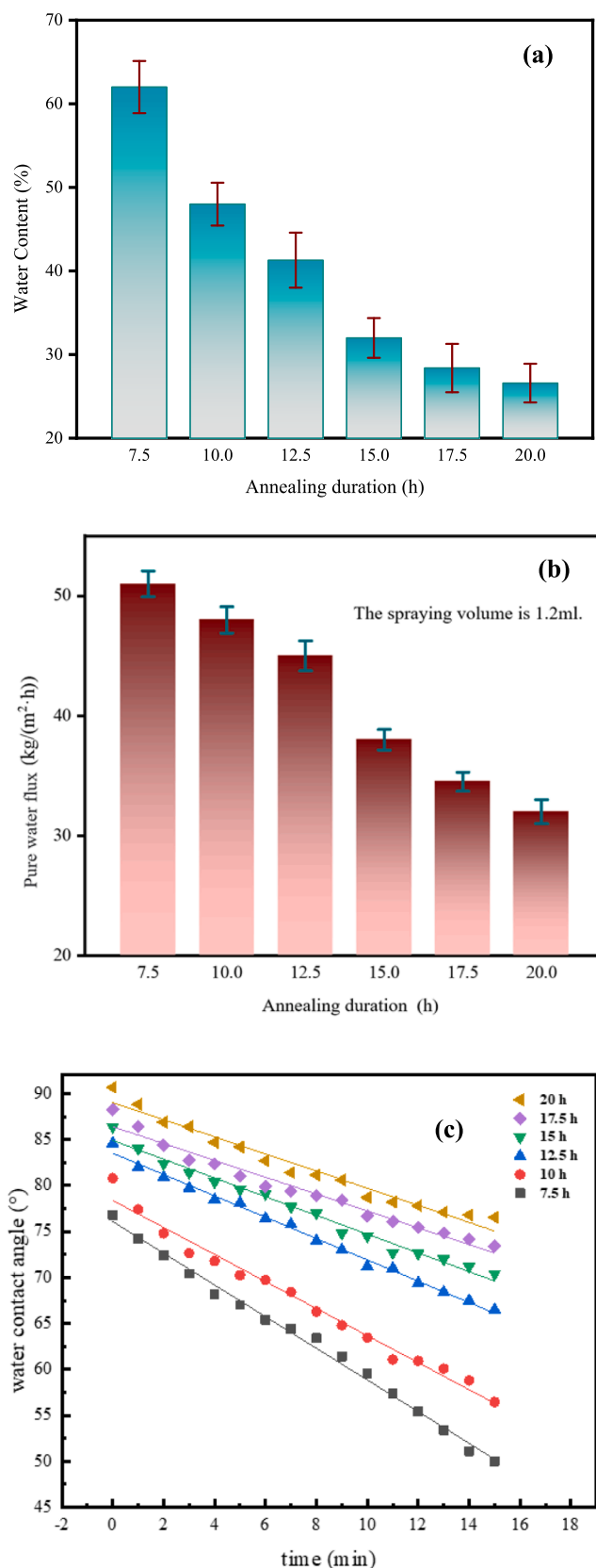


Fig. 6. The hydrophilicity of PFSA membranes at different post-treatment temperatures is different, where (a) is the water content, (b) is the pure water flux, and (c) is the dynamic water contact Angle.

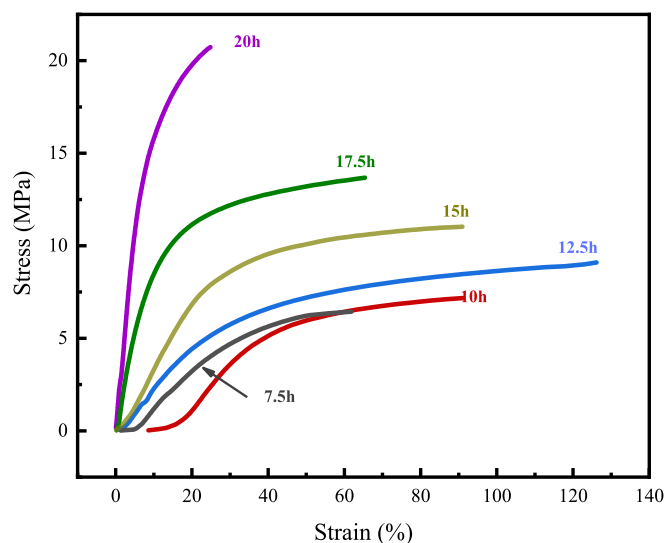


Fig. 7. DMA stretching curves of PFSA membranes with different annealing duration.

lower frequency, from 1061.6 cm^{-1} to 1055.7 cm^{-1} , and the group shift became less obvious after 4 h soaking.

Fig. 8(b₁) and (b₂) shows the changes of XRD diffraction peaks of PFSA membrane with annealing duration of 12.5 h before and after soaking in H_2SO_4 solution at 70°C for 72 h, which can be obtained by equations (3) and (5). After soaking, the crystallinity of PFSA membrane increases from 16.81 % to 17.95 %, and the half-peak width hardly changes. As a result, the grain size is also around 3.13 nm.

As can be seen from Fig. 8(c₁) and (c₂), the water contact angle of the membrane increases somewhat before and after soaking H_2SO_4 , and the hydrophilicity of the membrane decreases.

When hydrogen bonds are formed in the membrane, the average density of the electron cloud increases, resulting in a decrease in the group frequency of the stretching vibration, and the absorption summit of the proton donor appears to shift toward the lower wave number segment. At the same time, the order of the amorphous region is improved in the XRD diffraction peak, resulting in an increase in crystallinity. As the $-\text{SO}_3^-$ group absorption peak of PFSA membrane moves to lower frequency and increases crystallinity in the immersion of H_2SO_4 solution, we can speculate that under the action of H_2SO_4 at 70°C , new hydrogen bonds are formed inside PFSA membrane, which leads to the movement of the $-\text{SO}_3^-$ absorption peak to the lower wave number segment and the increase of crystallinity. At the same time, the hydrophilicity of the membrane decreased. In addition, the formation of hydrogen bonds was more obvious when the soaking time was less than 4 h, and the shift of infrared absorption peak was not obvious after 4 h, which indicated that H_2SO_4 had a limited role in promoting hydrogen bond formation in PFSA membrane.

Fig. 8(d₁) and (d₂) show that the membrane thickness of the dense layer did not change much after the acid concentration test, indicating that the dense layer did not lose much mass during the acid concentration test. As shown in Fig. 8 (e₁), the thermogravimetric process of PFSA membrane can be divided into the following four stages [41]: Water removal in the membrane mainly occurs at $25 \sim 200^\circ\text{C}$, and the mass of PFSA membrane is reduced by 2.45 %; At $200\text{--}280^\circ\text{C}$, the C-S bond on the side chain will be broken, resulting in the formation of $-\text{CF}_2$ -free radicals and $-\text{SO}_3\text{H}$ free radicals, resulting in the generation of CO_2 and SO_2 gas, and 0.85 % mass loss of PFSA membrane. In the temperature range of $280 \sim 375^\circ\text{C}$, the mass loss of resin is 10.25 %, and the DTG curve has an obvious peak in this temperature range. The main chain cracking occurred mainly in the temperature range of $375 \sim 550^\circ\text{C}$, and the mass loss of the inner membrane reached 77.35 %, and

the DTG curve produced a more obvious peak in this temperature range. In Fig. 8 (e₁) and (e₂) respectively show the TG curves of PFSA membrane before and after immersion in H_2SO_4 solution. It is not difficult to see that there is no significant difference in the TG process of PFSA membrane before and after immersion in sulfuric acid, and the above four stages still occur, and the weight loss peaks before and after immersion are basically the same.

In summary, under the condition of sulfuric acid immersion at 70°C , PFSA membrane density is intact. In addition, the enhancement of hydrogen bond in this condition leads to the increase of hydrophilicity.

3.2.2. Concentration of H_2SO_4 solution

Fig. 9(a) shows the flux and H_2SO_4 retention of a feed solution with an initial concentration of 5 wt% in the pervaporation of PFSA/PTFE/PP composite membrane. During the 19 h operation of acid concentration, the retention rate remained at 99.9 %. After the PV operation, the solute on the surface and inside of the composite membrane was washed and dried, and the composite membrane could pass the leak detection test. This shows that the density of the membrane has remained intact and can have a good barrier effect on the solute. Fig. 9(b) shows the concentration change measured by the feed. The results show that after PV operation for 19 h, the removal water of the composite membrane is 300 g, and the H_2SO_4 of 5 wt% is concentrated to 20 wt%, where the actual area of the composite membrane is 3.46 cm^2 .

In the PV concentration test of H_2SO_4 solution of the composite membrane, the water flux was $57.43\text{ kg}/(\text{m}^2\cdot\text{h})$ in the first 0.5 h of the test run, and decreased to $49.52\text{ kg}/(\text{m}^2\cdot\text{h})$ in 0.5 ~ 1h, and then slowly decreased at a regular rate. As the feed liquid is continuously concentrated and the concentration increases, the vapor partial pressure of water molecules decreases, and the pressure drive of water molecules becomes smaller, thus reducing the water flux. In addition, it is concluded in Section 3.2.1 that the immersion of H_2SO_4 solution can promote the formation of hydrogen bonds in PFSA, resulting in the decrease of hydrophilicity and water flux of the composite membrane. Therefore, we tested the pure water flux of the composite membrane during the PV concentration process, in order to exclude the influence of the change of solution concentration. After testing the acid flux every half hour or one hour, the PV composite membrane in the concentration operation was taken out and washed and dried. The pure water flux of the membrane at this time was tested and compared with the initial pure water flux, which was used as the reference amount for the change of hydrophilicity of the composite membrane in the acid concentration test.

As shown in the figure above, after the pervaporation experiment of the composite membrane with 5 wt% H_2SO_4 as the feed liquid was run for 0.5 h, the pure water flux decreased from the initial $45 \pm 1.2\text{ kg}/(\text{m}^2\cdot\text{h})$ to $33.05 \pm 0.65\text{ kg}/(\text{m}^2\cdot\text{h})$, and then remained stable at about $32\text{ kg}/(\text{m}^2\cdot\text{h})$. The rapid decline of initial water flux in the PV acid concentration test is similar to the change trend of pure water flux in the composite membrane during the PV concentration process, which indicates that the sudden decline of water flux in the initial PV acid concentration is not only affected by the concentration of feed liquid, but also related to the decrease of membrane hydrophilicity, resulting in a sudden decline of initial water flux. However, whether the internal structure of the membrane is stable at 0.5 h of acid concentration still needs further investigation.

As shown in Fig. 9(d), when the composite membrane was immersed in 20 wt% H_2SO_4 solution at 70°C , the pure water flux decreased from the initial $45.18\text{ kg}/(\text{m}^2\cdot\text{h})$ to $32.18\text{ kg}/(\text{m}^2\cdot\text{h})$ after about 2.5 h and fluctuated slightly at about $32\text{ kg}/(\text{m}^2\cdot\text{h})$. This is similar to the variation trend of pure water flux of the composite membrane in the PV process shown in Fig. 9(c). However, it takes a long time for the former to reach the inflection point and the stable state. This is because during the immersion of H_2SO_4 solution, the movement speed of H_2SO_4 is slow, the transformation speed of membrane structure is also slow, and the pure water flux appears stable at about 2.5 h. In the PV process, the

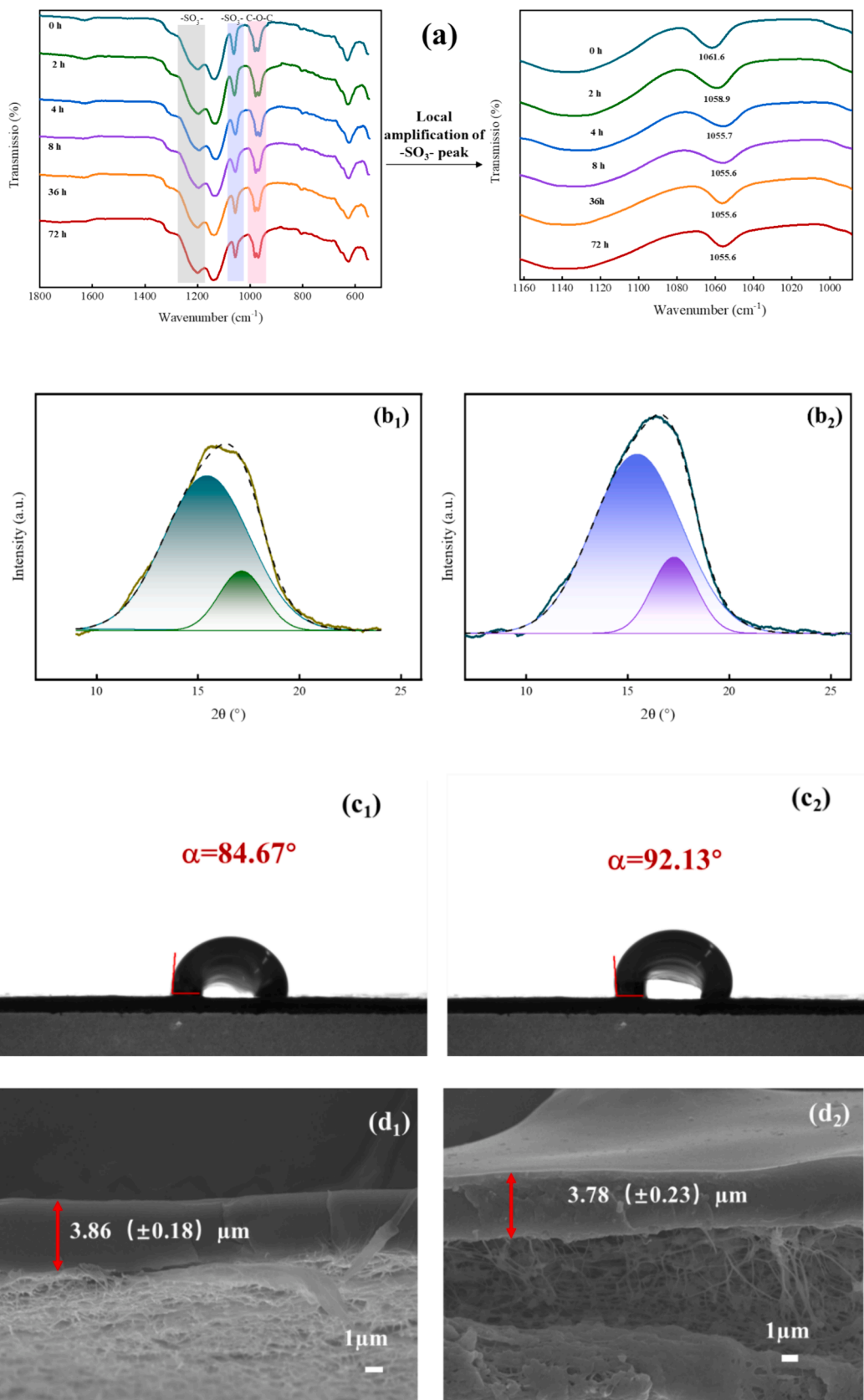


Fig. 8. Changes of structure and properties of PFSA membrane before and after soaking in H₂SO₄ solution, Where (a) is the change of infrared spectrum, (b₁) and (b₂) are the changes of crystallization, (c₁) and (c₂) are the changes of the membrane contact Angle, (d₁) and (d₂) are the changes of SEM fracture surface and (e₁) and (e₂) are the changes of the TG.

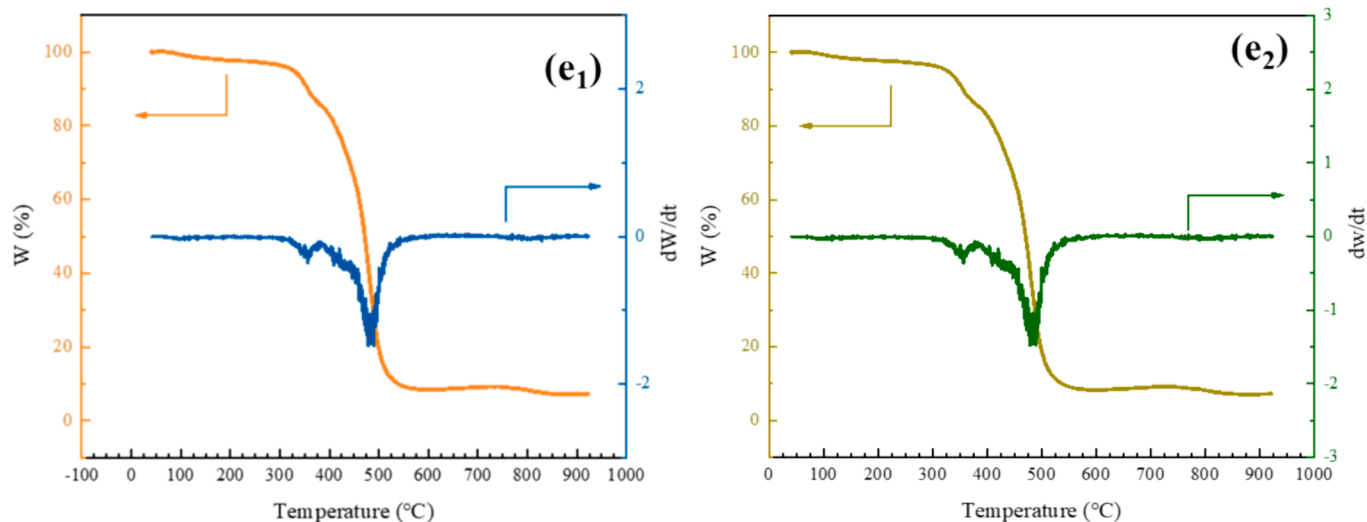


Fig. 8. (continued).

permeation of the membrane is kept in a vacuum state, and the material liquid is in a turbulent state on the surface of the membrane, which can accelerate the motion speed of H_2SO_4 , thus accelerating the structural transformation process of the membrane. Therefore, the stable state of pure water flux appears at about 0.5 h.

Fig. 9(c) and Fig. 9(d) can be used as the time comparison of hydrophilicity changes between composite membrane acid soaking and PV acid concentrated membrane. When the density of the membrane remains intact in the PV process, the sulfuric acid soaking and sulfuric acid concentration processes of the composite membrane have very similar effects on the dense layer. Therefore, this comparison relationship can be used as an approximate comparison diagram of the membrane structure changes leading to the change of the hydrophilicity of the membrane and can be used to approximate the XRD pattern of the PFSA layer in the composite membrane at a certain time point in the PV concentration process. When the XRD pattern of the dense layer at a certain time point in the PV process needs to be obtained, the immersion time corresponding to the same pure water flux of the composite membrane can be found, and the XRD pattern of the PFSA layer at a certain time node in the PV process can be approximately derived by soaking the intrinsic PFSA membrane prepared under the same conditions for the same time after testing.

It can be seen from Fig. 10 and Table 3 that the crystallinity of PFSA membrane in H_2SO_4 solution tends to increase, and there is little difference between the crystal structure of the membrane soaked for 2.5 h and that of the membrane soaked for 6 h. During the soaking process of H_2SO_4 solution, the effect on PFSA membrane mainly occurs in the first 2.5 h. Comparing Fig. 9(c) and Fig. 9(d), the internal structure of PFSA membrane after soaking for 2.5 h is approximately equal to the structure of the dense layer of the composite membrane at 0.5 h in the PV acid concentration test. It can be understood that in the acid concentration test, the change of the crystalline structure of the dense layer of the composite membrane mainly occurs in the first 0.5 h, and there is little change in the subsequent test. When the PV acid concentration test was carried out for 0.5 h, the crystallinity of the dense layer increased from the original 16.81 % to 17.95 %.

With the increase of crystallinity, the water permeability of the composite membrane decreases, the pure water flux of the composite membrane decreases, and the water flux drops sharply at the beginning of the acid concentration process. The crystalline structure of the composite membrane in the PV acid concentration test for 0.5 h reached a relatively stable state, and the hydrophilicity also tended to be stable. After 0.5 h of acid concentration test, the water flux in acid

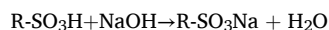
concentration process decreased slowly due to the increasing concentration of feed liquid.

If we want to reduce the sudden drop of flux in the early stage of the composite membrane during the H_2SO_4 concentration pervaporation operation, the composite membrane can be treated with acid first, and the composite membrane can be immersed in 20 wt% H_2SO_4 solution at 70°C for about 3 h to complete the transformation of the crystallization properties of the membrane.

3.3. Evaluation of alkali resistance of composite membrane

3.3.1. Effect of NaOH on the structure of dense layer

The element composition in the PFSA membrane is different before and after soaking NaOH, and the membrane itself does not contain Na element. Immersion in caustic soda solution leads to a transformation process, which converts H in $-\text{SO}_3\text{H}$ into Na, and the dense layer transforms from PFSA-H into PFSA-Na, that is, H-Na transformation. The transformation process can be expressed as follows:



The above process can be concluded from Fig. 11 and Table 4.

Compared with $-\text{SO}_3\text{Na}$ in PFSA-H, the $-\text{SO}_3\text{H}$ in PFSA-H can form stronger hydrogen bonds with water molecules and has stronger bonding ability with water molecules. Therefore, the H-Na transformation process will result in a decrease in the hydrophilicity of the composite membrane.

At the same time, it can be seen from the thermogravimetric diagrams before and after immersion that PFSA-Na has better thermal stability than PFSA-H [41], there is no DTG weight loss peak in the range of $280 \sim 375^\circ\text{C}$, polymer decomposition occurs at about 415°C , and the peak of DTG curve occurs at $415 \sim 550^\circ\text{C}$. It also shows that the transformation process has no impact on the main structure of PFSA layer.

As the H-Na transformation process can occur in the PFSA membrane in NaOH solution, H^+ in the membrane is replaced by Na^+ . Under the influence of counterion (Na^+), the C-O-C absorption peak in the PFSA-Na molecule weakens at this band, and $-\text{SO}_3^-$ is affected by the electrostatic field of adjacent ion pairs due to the H-Na transformation. The S-O bond produces induced polarization effect, and the absorption peak of PFSA-Na in this band can move 5 cm^{-1} toward the high frequency relative to the absorption peak of PFSA-H, which is shown as the absorption peak of $-\text{SO}_3^-$ near 1057.8 cm^{-1} moves from the high frequency to 1062.8 cm^{-1} .

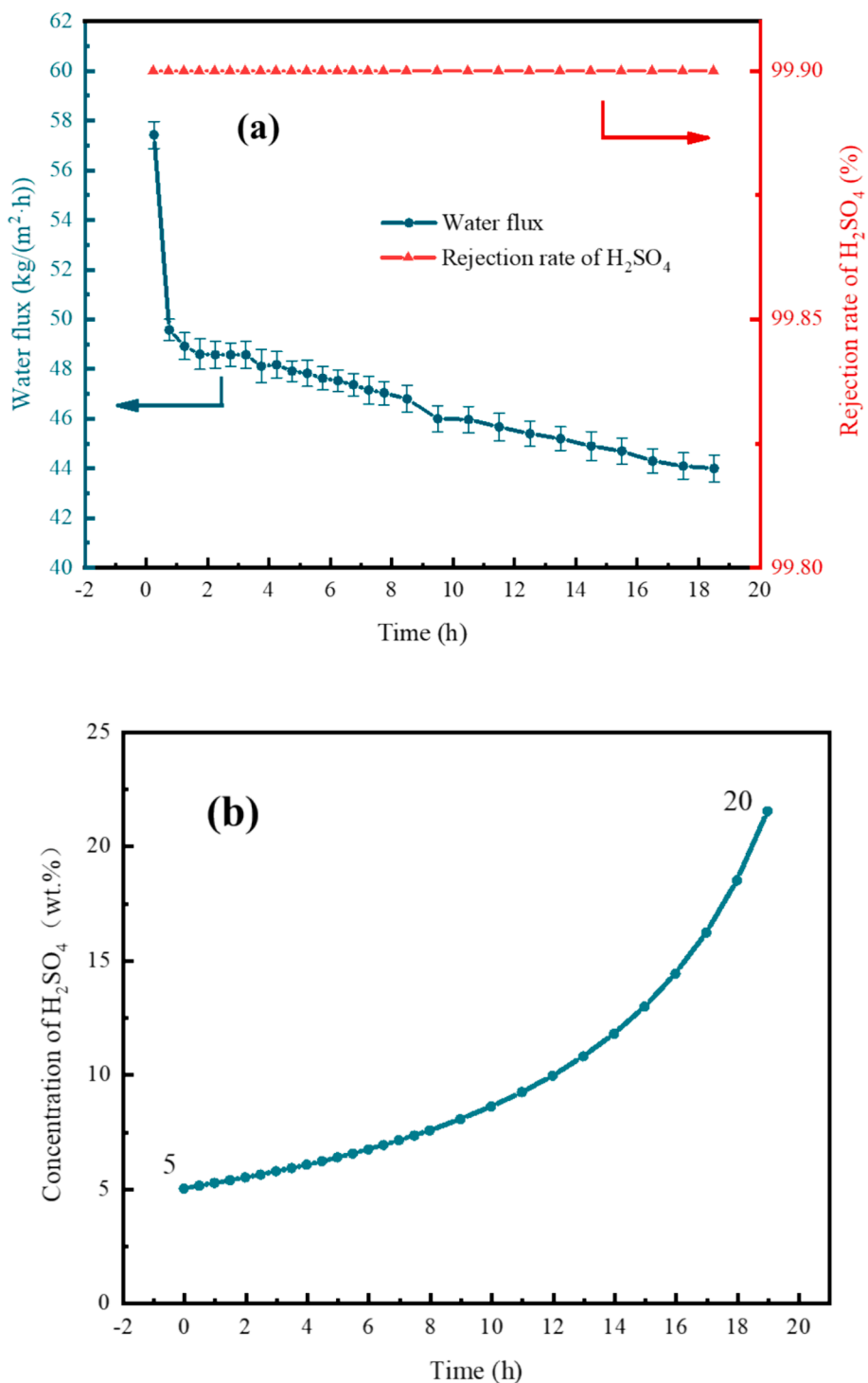


Fig. 9. PV concentration process of H₂SO₄ solution, where (a) is flux and retention, where (b) is change of feed solution concentration, where (c) is change of pure water flux of the composite membrane, where (d) is change of pure water flux of the composite membrane during H₂SO₄ immersion.

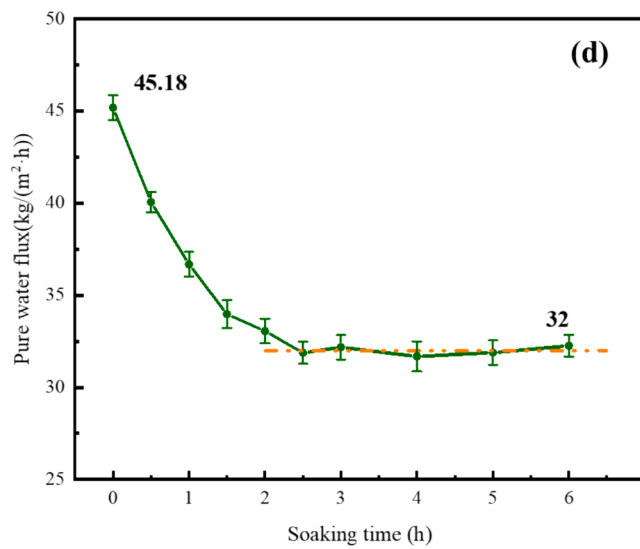
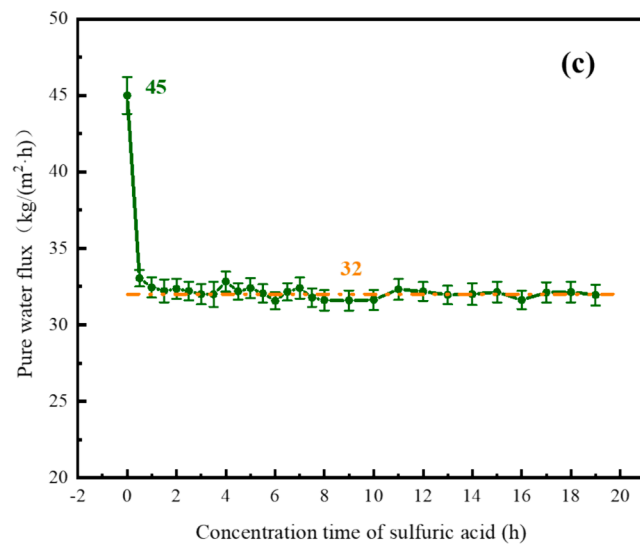


Fig. 9. (continued).

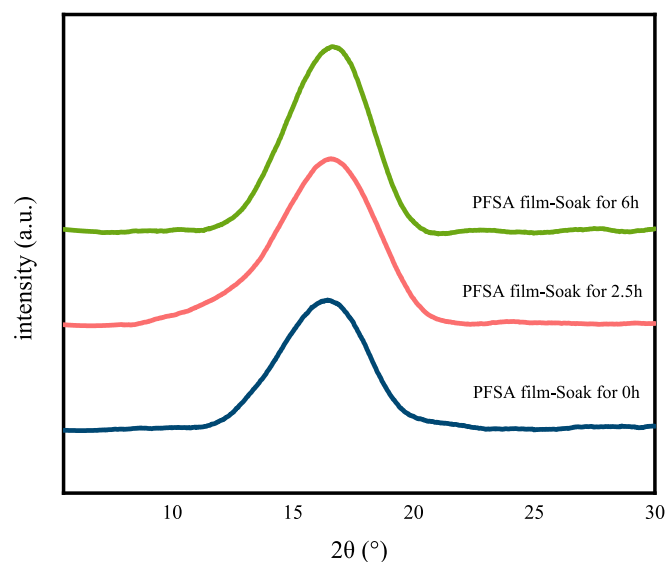


Fig. 10. The XRD patterns of PFSA membrane before and after immersion in H_2SO_4 solution were changed.

Table 3

The crystallization degree of PFSA membrane was changed before and after immersion in H_2SO_4 solution.

Soaking time (h)	degree of crystallinity (%)	Half-peak width (°)	the average size of grains (nm)
0	16.81	2.63	3.13
2.5	17.95	2.62	3.14
6	17.95	2.62	3.14

However, the group moving wave number in Fig. 12(a) is larger than that of 5 cm^{-1} , indicating that immersion of NaOH solution has other effects on PFSA membrane.

Fig. 12(b₁) and (b₂) show the changes of XRD diffraction peaks of PFSA membrane with annealing duration of 12.5 h before and after soaking in NaOH solution at 70°C for 72 h. It can be calculated by equations (3) and (5) that the crystallinity of PFSA membrane after soaking decreases from 16.81 % to 16.02 %, and the half-peak width hardly changes. Therefore, the grain size is also about 3.13 nm. In addition, it can be seen from the contact Angle changes of PFSA membrane in Fig. 12(c₁), (c₂) and (c₃) that the hydrophilicity of the membrane increases firstly and then decreases.

When the hydrogen bond in the membrane is destroyed, the average density of the electron cloud is weakened, the group frequency of the stretching vibration is increased, the absorption peak of the proton donor is shifted to the high wave number segment, and the order of the amorphous region in the membrane is also reduced, which is manifested by the decrease of crystallinity and the increase of hydrophilicity. At the same time, H-Na transition decreased hydrophilicity. It can be speculated that the shift of $-SO_3^-$ group absorption peak to higher wave number and the decrease of crystallinity in PFSA membrane maybe due to the effect of NaOH on PFSA membrane, which leads to the destruction of hydrogen bonds in the membrane. The attack of hydrogen bond combined with H-Na transformation caused the $-SO_3^-$ group of PFSA-Na to move from 1057.8 cm^{-1} to 1064.2 cm^{-1} . In addition, it can be seen from Fig. 12(d₁) and (d₂) that the membrane thickness is not affected by NaOH solution.

3.3.2. Concentration NaOH of solution

As can be seen from Fig. 13(a), when NaOH solution was used as the feed liquid for the PV experiment, the solute retention rate of the

composite membrane remained at 99.9 % during the 19 h running time. After the concentration operation of NaOH solution was completed, the composite membrane was washed with ultrapure water to clean the solute on the surface and inside of the composite membrane and dried, and the composite membrane could pass the leak detection test. This indicates that the densification of the dense layer is not destroyed by NaOH solution during the whole operation process, and it can remain intact during the concentration process, and it has a good tolerance to 5–20 wt% NaOH solution at 70°C . Fig. 13(b) shows the concentration change measured by feeding material. The results show that, under the condition that the actual working area of the composite membrane is 3.46 cm^2 , after PV operation for 19 h, the water removal is 300 g during the operation, and the concentration of NaOH solution is concentrated from the initial 5 wt% to 20 wt%.

In the whole process of NaOH solution concentration, the water flux of the composite membrane was unstable in the early stage. The overall trend of water flux was first rising, then plummeting, and then slowly declining. The overall trend indicated that the microstructure of the membrane changed during the alkali concentration operation, which led to the fluctuation of its hydrophilicity. As mentioned in the previous section, the destruction of hydrogen bonds and H-Na transformation work together to cause the hydrophilicity of PFSA membrane to first increase and then decrease. This is similar to the trend of water flux change in Fig. 13(a), but the specific time node of membrane structure change in the PV process needs to be further explored. To eliminate the influence of solution concentration on water flux, pure water flux test was carried out on the composite membrane in the process of NaOH concentration by pervaporation. After each operation stage (every 0.5 h or 1 h), the composite membrane in the concentration was taken out, washed and dried to determine its pure water flux at the moment, and compared with the initial pure water flux, the change trend of its hydrophilicity was obtained.

As shown in Fig. 13(c), the hydrophilicity of the composite membrane changes due to the influence of NaOH solution on the internal structure during the early concentration process, resulting in the hydrophilicity increasing first and then decreasing. The hydrophilicity does not fluctuate much after about 8 h, but it is unknown whether the internal structure of the membrane is in a stable state at this time.

Fig. 13(d) shows that the pure water flux of the composite membrane soaked in 20 wt% NaOH solution at 70°C changes with the soaking time, and the pure water flux rises from the initial $45.06 \pm 0.86\text{ kg}/(\text{m}^2\cdot\text{h})$ to $59.69 \pm 0.45\text{ kg}/(\text{m}^2\cdot\text{h})$. After 12 h, it decreased to about $42.5\text{ kg}/(\text{m}^2\cdot\text{h})$ and remained stable, which was similar to the change trend of pure water flux in the PV process as shown in Fig. 13(c). However, the former took a longer time to reach the inflection point and stable state, which was due to the slower NaOH movement speed and slower membrane structure transformation speed during the immersion process of alkali solution compared with the concentration process of PV alkali. The pure water flux is stable at about 12 h, and the pure water flux is stable at about 8 h in the PV process. Fig. 13(c) and Fig. 13(d) are the time comparison diagrams of hydrophilicity changes of the composite membrane alkaline immersion and PV alkali concentrated membrane, which are the same as inferred in Section 3.3.2. The XRD pattern of the PFSA layer at a certain time node in the PV process can be approximately obtained through the comparison relationship between the two.

Fig. 14 shows the decreasing trend of crystallinity of the composite membrane when exposed to NaOH solution, and Table 5 can be obtained from the peak fitting calculation. The crystal structure of the membrane soaked in NaOH solution for 8 h had little difference from that soaked for 18 h. It can be understood that after soaking for 8 h, NaOH had almost no effect on the crystallinity of the membrane. It can be seen from the comparison of Fig. 13 that the internal structure of PFSA membrane after soaking for 8 h is approximately equal to the structure of the dense layer of the composite membrane at 4 h in the PV concentration test for NaOH solution. It can be understood that in the alkali concentration test, the change of the crystalline structure of the dense layer of the

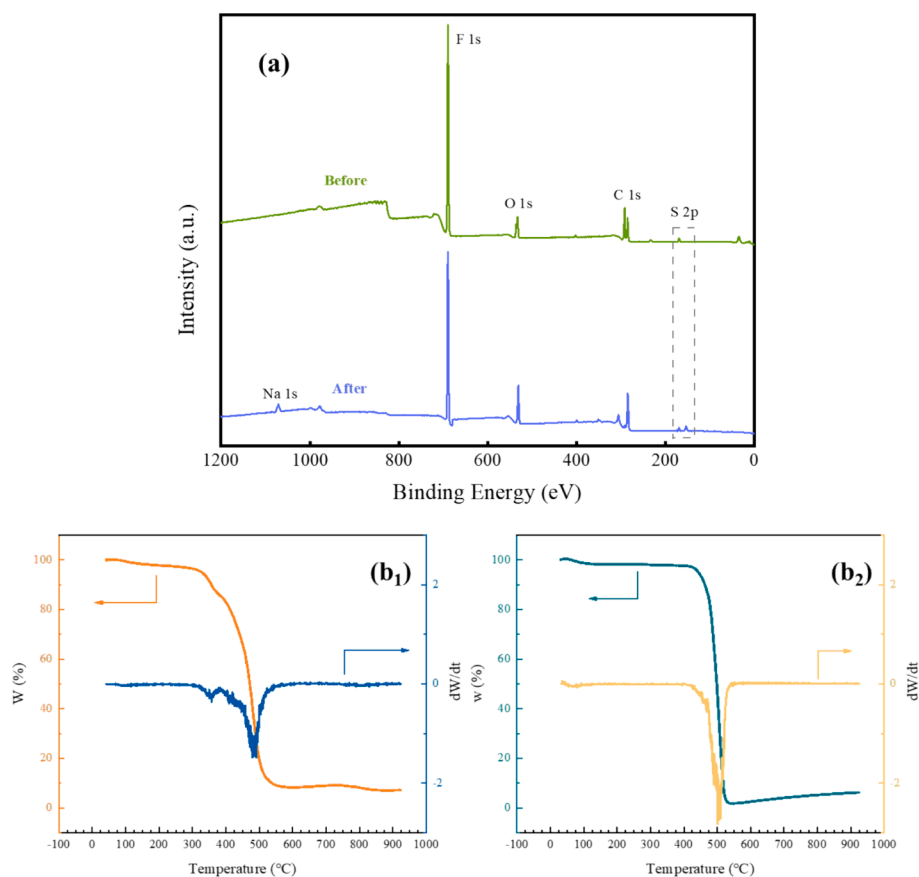


Fig. 11. Changes in PFSA membrane before and after immersion in NaOH solution for 72 h, where (a) is of change of elements, (b₁) and (b₂) are the changes of the TG.

Table 4

Changes of elements in PFSA membrane before and after immersion in NaOH solution for 72 h.

Sample	Elemental Composition				
	C	F	O	S	Na
Before soaking	33.3	58.69	6.31	1.7	0
After soaking	32.7	57.08	7.12	1.52	1.58

composite membrane mainly occurs in the first 4 h, and there is little change in the subsequent period. When the PV concentration test was carried out for 4 h, the crystallinity of the dense layer decreased from the original 16.81 % to 16.02 %.

At the same time, we know that the concentration process of NaOH solution is also accompanied by the H-Na transformation process, which plays a certain role in reducing the hydrophilicity of PFSA membrane, which also leads to the reduction of pure water flux. As the concentration process progresses, the limitation of hydrogen bonding and the completion of transformation will eventually lead to the stability of pure water flux.

In conclusion, in the first 2.5 h concentration test of NaOH solution, the decrease of crystallinity caused by hydrogen bond destruction plays a leading role in affecting the properties of dense layer, and the hydrophilicity increases. Due to the limited function of hydrogen bonding, the change of crystallinity gradually decreases at 2.5 h, at which time the transition plays a leading role in the influence of the dense layer, and the hydrophilicity of the dense layer decreases. As shown in Fig. 13, when the PV concentration test is carried out within 2.5–8 h, the pure water flux shows a decreasing trend, which is like the change trend of the water flux in the alkali concentration test. The combination of

crystallinity and H-Na transition results in the change of structure and hydrophilicity in the early stage of the composite membrane, which is manifested by the change of water flux in alkali concentration test. After 8 h, the membrane structure no longer fluctuates greatly, and the pure water flux tends to be stable. Currently, the water flux in the concentration test only decreases slowly under the influence of the concentration of the feed liquid.

In order to reduce the flux fluctuation in the early stage of PV concentration process of NaOH solution, the composite membrane can be soaked in alkaline solution first, that is, the composite membrane is immersed in 20 wt% NaOH solution and soaked at 70°C for about 12 h, so that the crystallinity of the membrane and H-Na transformation can be completed.

4. Conclusion

In this paper, PFSA/PTFE/PP composite membrane was prepared by spraying method, and dense layers with different crystallization properties were obtained by controlling the annealing time during the post-treatment process, so as to control the hydrophilicity and acid-base stability of PFSA layer. Finally, obtain the PV composite membrane with excellent acid-base concentration efficiency and acid-base resistance. The specific contents are as follows:

(1) The infiltration degree of the dense layer is controlled by adjusting the content of ethanol in the spray liquid, to adjust the interface bonding between the dense layer and PTFE microfiltration membrane and the water transport efficiency of the composite membrane, and finally determine the solvent ratio of the spray liquid to ethanol: water = 1:20.

(2) A composite membrane with a pure water flux of 45 ± 1.2 kg/(m²·h) and a retention rate of 99.9 % of acid and base was prepared by

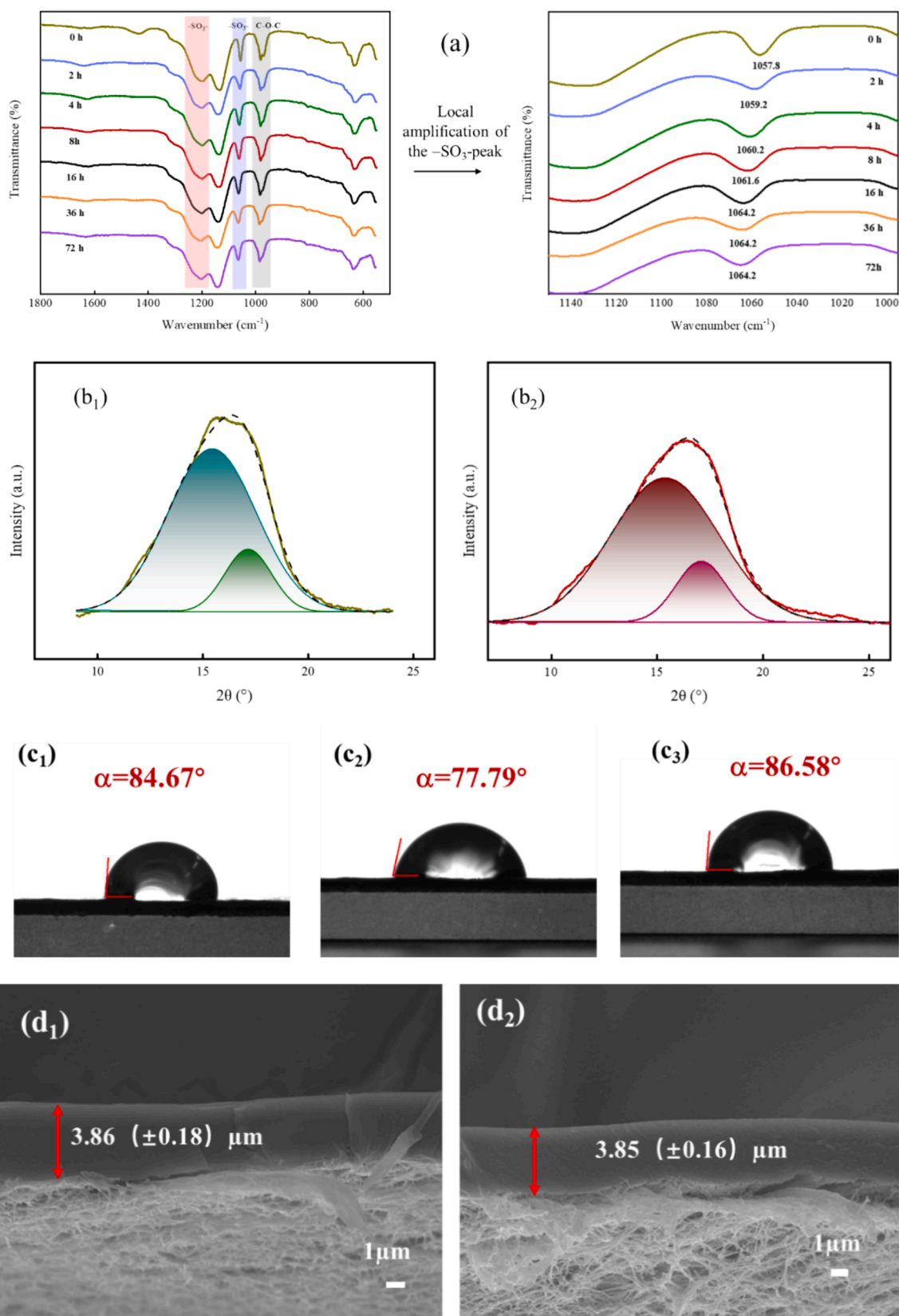


Fig. 12. Changes of structure and properties of PFSA membrane before and after soaking in NaOH solution, Where (a) is the change of infrared spectrum, (b₁) and (b₂) are the changes of crystallization, (c₁), (c₂) and (c₃) are the changes of the membrane contact Angle and (d₁) and (d₂) are the changes of SEM fracture surface.

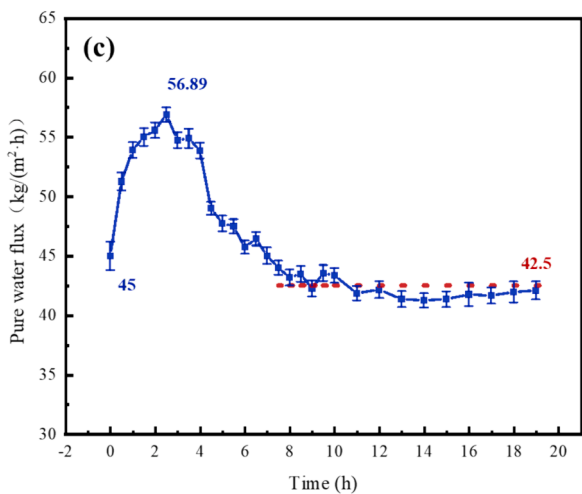
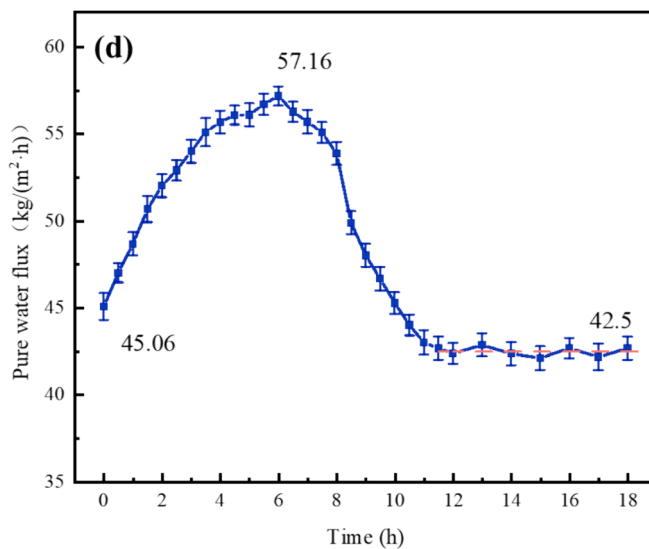
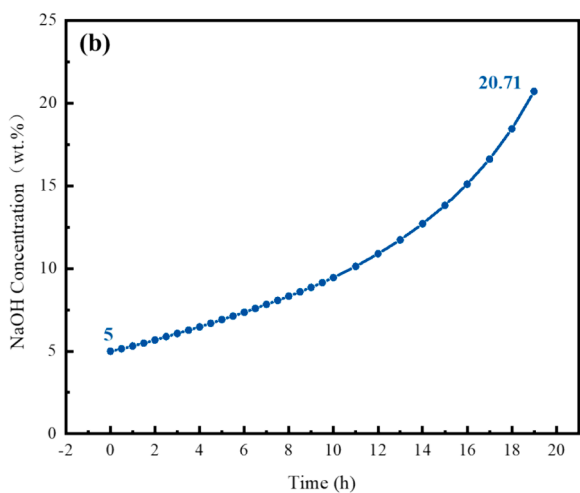
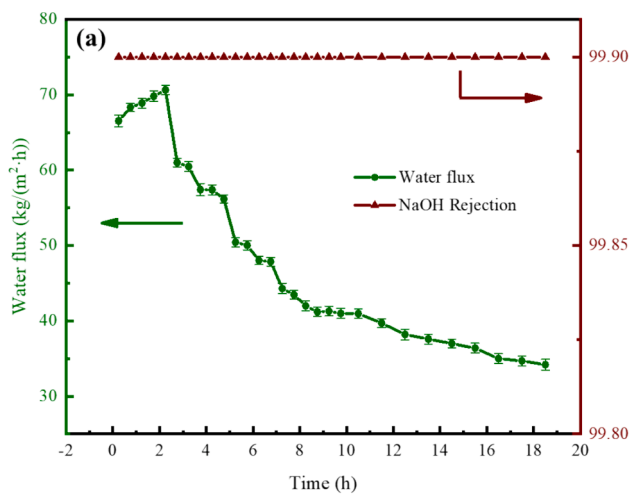


Fig. 13. PV concentration process of NaOH solution, where (a) is flux and retention, where (b) is change of feed solution concentration, where (c) is change of pure water flux of the composite membrane, where (dc) is change of pure water flux of the composite membrane during NaOH immersion.

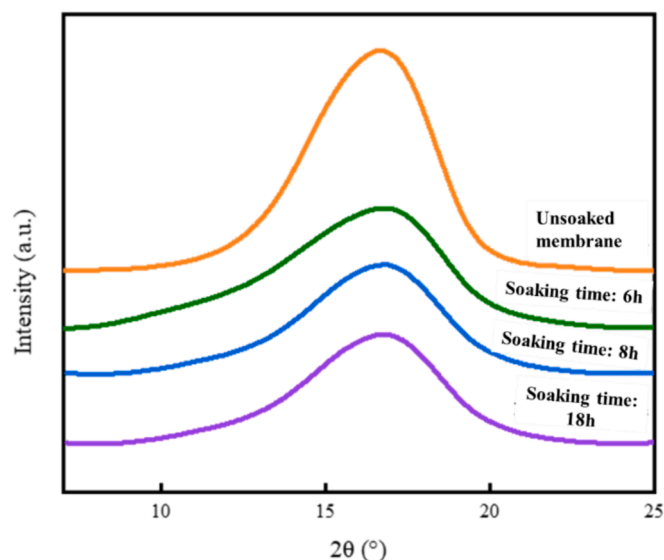


Fig. 14. The XRD patterns of PFSA membrane before and after immersion in NaOH solution were changed.

Table 5

Crystallization analysis of PFSA membrane before and after immersion in NaOH solution.

Annealing duration (h)	Degree of crystallinity (%)	Half-peak width (°)	The average size of grains (nm)
0	16.81	2.63	3.13
6	16.33	2.65	3.10
8	16.02	2.65	3.10
18	16.02	2.65	3.10

spraying process. After 19 h of PV operation, the stock solution was concentrated from 5 wt% to 20 wt%.

(3) Under the action of H_2SO_4 solution, there will be a slight increase in the crystallinity of PFSA layer in the early stage, which will lead to a decrease in the membrane flux. The original pure water flux of the composite membrane is $45 \pm 1.2 \text{ kg}/(\text{m}^2\cdot\text{h})$, and the pure water flux of the composite membrane is reduced to about $32 \text{ kg}/(\text{m}^2\cdot\text{h})$ after 0.5 h PV operation of H_2SO_4 solution.

(4) Under the action of NaOH solution, PFSA layer will have a slight decrease in crystallinity in the early stage, which will lead to an increase in the flux of the composite membrane; At the same time, NaOH can lead to the transition from PFSA-H to PFSA-Na, which in turn leads to the reduction of flux. Together, the pure water flux of the composite membrane with a membrane pure water flux of $45 \pm 1.2 \text{ kg}/(\text{m}^2\cdot\text{h})$ fluctuates around $40 \text{ kg}/(\text{m}^2\cdot\text{h})$ after PV operation of NaOH solution for 8 h.

Declaration of competing interest

The authors declare that they have no known competing financial interests or personal relationships that could have appeared to influence the work reported in this paper.

Data availability

Data will be made available on request.

Acknowledgment

The first author thanks Mr. Chenghao Niu for his help in the

experiment and the revision of the paper. The first author thanks Mr. Rui Zhang for the guidance of the experiment. We also gratefully acknowledge the support from the NERC204 project (Changzhou Key Laboratory of Biomass Green, Safe & High Value Utilization), which significantly contributed to the success of this research.

References

- [1] E. Paquay, A. Clarinval, A. Delvaux, et al., Applications of electro dialysis for acid pickling waste water treatment, *Chem. Eng. J.* 79 (3) (2000) 197–201.
- [2] F.W. Sousa, M.J. Sousa, I.R.N. Oliveira, et al., Evaluation of a low-cost adsorbent for removal of toxic metal ions from wastewater of an electroplating factory, *J. Environ. Manage.* 90 (11) (2009) 3340–3344.
- [3] C. Sanchez-Ruiz, S. Martinez-Royano, I. Tejero-Monzon, An Evaluation of the efficiency and impact of raw wastewater disinfection with peracetic acid prior to ocean discharge, *Water Sci. Technol.* 32 (7) (1995) 159–166.
- [4] J.E. Holguin-Gonzalez, G. Everaert, P. Boets, et al., Development and application of an integrated ecological modelling framework to analyze the impact of wastewater discharges on the ecological water quality of rivers, *Environ. Model. Softw.* 48 (10) (2013) 27–36.
- [5] M. Zhang, X.M. Li, Impact of acid deposition on the soil acidification of Mt Taishan, *J. Shandong Univ.* 45 (1) (2010) 36–40.
- [6] G. Zhang, Q. Zhang, K. Zhou, Acid recovery from waste sulfuric acid by diffusion dialysis, *J. Cent. South Univ. Technol.* 6 (2) (1999) 103–106.
- [7] C. Chen, H. Xie, Y. Jiang, et al., Influence of hydrophobic components tuning of poly (aryl ether sulfone) s ionomers based anion exchange membranes on diffusion dialysis for acid recovery, *J. Membr. Sci.* 636 (2021) 119562.
- [8] B. Liu, Y. Duan, T. Li, et al., Nanostructured anion exchange membranes based on poly (arylene piperidinium) with bis-cation strings for diffusion dialysis in acid recovery, *Sep. Purif. Technol.* 282 (2022) 120032.
- [9] F. Ilhan, H.A. Kabuk, U. Kurt, et al., Recovery of mixed acid and base from wastewater with bipolar membrane electro dialysis—a case study, *Desalin. Water Treat.* 57 (11) (2016) 5165–5173.
- [10] X. Liu, Y. Shan, Q.P.H. Zhang, Application of metal organic framework in wastewater treatment, *Green Energy Environ.* 8 (3) (2023) 698–721.
- [11] S. Yu, H. Qian, J. Liao, et al., Proton blockage PVDF-co-HFP-based anion exchange membrane for sulfuric acid recovery in electro dialysis, *J. Membr. Sci.* 653 (2022) 120510.
- [12] H. Xu, X. Ji, L. Wang, et al., Performance study on a small-scale photovoltaic electro dialysis system for desalination, *Renew. Energy* 154 (2020) 1008–1013.
- [13] E. Paquay, A. Clarinval, A. Delvaux, et al., Applications of electro dialysis for acid pickling wastewater treatment, *Chem. Eng. J.* 79 (3) (2000) 197–201.
- [14] D.C. Zhang, L. Liu, D.M. Guan, et al., Study on treatment of smelting contaminated acid by evaporation condensing process, *Adv. Mat. Res.* 2951 (2014) 564–569.
- [15] Y.I. Zheng, Y.L. Peng, C.H. Li, Treatment of acid mine drainage by two-step neutralization, *J. Cent. South Univ.* 42 (5) (2011) 1215–1219.
- [16] X. Zhang, J. Scott, et al., Advanced treatment of hydrothermal liquefaction wastewater with nanofiltration to recover carboxylic acids, *Environ. Sci., Water Res. Technol.* 4 (4) (2018) 520–528.
- [17] T. Gun, J. Dan, Purification of alkaline cleaning solutions from the dairy industry using membrane separation technology, *Desalination* 119 (1–3) (1998) 21–29.
- [18] A. Fahmy, D. Mewes, K. Ohlrogge, Novel pervaporation technology using absorption refrigeration for vapor removal, *AIChE J* 48 (11) (2010) 2518–2523.
- [19] S.K. Myasnikov, A.D. Uteshinsky, N.N. Kulov, Hybrid of pervaporation and condensation-distillation crystallization: a new combined separation technology, *Theor. Found. Chem. Eng.* 37 (6) (2003) 527–532.
- [20] C. Cannilla, G. Bonura, F. Frusteri, Potential of pervaporation and vapor separation with water selective membranes for an optimized production of biofuels—a review, *Catalysts* 7 (6) (2017) 187.
- [21] X. Feng, R.Y.M. Huang, Liquid separation by membrane pervaporation: A review, *Ind. Eng. Chem. Res.* 36 (4) (1997) 1048–1066.
- [22] Q. Wang, Y. Lu, N. Li, Preparation, characterization and performance of sulfonated poly(styrene-ethylene/butylene-styrene) block copolymer membranes for water desalination by pervaporation, *Desalination* 390 (2016) 33–46.
- [23] G. Jyoti, A. Keshav, J. Anandkumar, Review on Pervaporation: Theory, Membrane Performance, and Application to Intensification of Esterification Reaction, *J. Eng.* 2015 (2015) 927068.
- [24] L.M. Vane, Review of pervaporation and vapor permeation process factors affecting the removal of water from industrial solvents, *J. Chem. Technol. Biotechnol.* 95 (3) (2020) 495–512.
- [25] S. Fan, Z. Xiao, M. Li, et al., Pervaporation performance in PDMS membrane bioreactor for ethanol recovery with running water and air as coolants at room temperature, *J. Chem. Technol. Biotechnol.* 92 (2) (2017) 292–297.
- [26] Y. Li, E.R. Thomas, M.H. Molina, et al., Desalination by membrane pervaporation: A review, *Desalination* 547 (2023) 116223.
- [27] M. Amirilargani, B. Sadatnia, Poly (vinyl alcohol)/zeolitic imidazolate frameworks (ZIF-8) mixed matrix membranes for pervaporation dehydration of isopropanol, *J. Membr. Sci.* 469 (2014) 1–10.
- [28] J. Sun, X. Qian, Z. Wang, et al., Tailoring the microstructure of poly (vinyl alcohol)-intercalated graphene oxide membranes for enhanced desalination performance of high-salinity water by pervaporation, *J. Membr. Sci.* 599 (2020) 117838.
- [29] J. Meng, C.H. Lau, Y. Xue, et al., Compatibilizing hydrophilic and hydrophobic polymers via spray coating for desalination, *J. Mater. Chem. A* 8 (17) (2020) 8462–8468.

- [30] D. Qin, R. Zhang, B. Cao, et al., Fabrication of high-performance composite membranes based on hierarchically structured electrospun nanofiber substrates for pervaporation desalination, *J. Membr. Sci.* 638 (2021) 119672.
- [31] J. Wang, B. Cao, R. Zhang, et al., Spray-coated tough thin membrane composite membrane for pervaporation desalination, *Chem. Eng. Res. Des.* 179 (2022) 493–501.
- [32] B. Wang, Z. Cao, Acid-catalyzed reactions of twisted amides in water solution: competition between hydration and hydrolysis, *Chemistry* 17 (42) (2011) 11919–11929.
- [33] K. Cui, P. Li, R. Zhang, et al., Preparation of pervaporation membranes by interfacial polymerization for acid wastewater purification, *Chem. Eng. Res. Des.* 156 (2020) 171–179.
- [34] G. Bai, J. Xia, B. Cao, et al., Fabrication of high-performance pervaporation composite membrane for alkaline wastewater reclamation, *Front. Chem. Sci. Eng.* 16 (5) (2022) 709–719.
- [35] K.A. Mauritz, R.B. Moore, State of Understanding of Nafion, *Chem. Rev.* 104 (10) (2004) 4535–4586.
- [36] Y. Luan, H. Zhang, Y. Zhang, et al., Study on structural evolution of perfluorosulfonic ionomer from concentrated DMF-based solution to membranes, *J. Membr. Sci.* 319 (1–2) (2008) 91–101.
- [37] Y. Luan, Y. Zhang, L. Li, et al., Perfluorosulfonic ionomer solution in N, N-dimethylformamide, *J. Appl. Polym. Sci.* 107 (5) (2008) 2892–2898.
- [38] Y. Luan, Y. Zhang, H. Zhang, et al., Annealing effect of perfluorosulfonated ionomer membranes on proton conductivity and methanol permeability, *J. Appl. Polym. Sci.* 107 (1) (2008) 396–402.
- [39] M. Agostini, Y. Aihara, T. Yamada, et al., A lithium-sulfur battery using a solid, glass-type P₂S₅-Li₂S electrolyte, *Solid State Ion.* (2013), 24448–51.
- [40] H. Song, H. Yu, L. Zhu, et al., Durable hydrophilic surface modification for PTFE hollow fiber membranes, *React. Funct. Polym.* 114 (2017) 110–117.
- [41] C.A. Wilkie, J.R. Thomsen, M.L. Mittleman, Interaction of poly (methyl methacrylate) and nafions, *J. Appl. Polym. Sci.* 42 (No. 4) (1991) 901–909.